

Supporting Information

Zwanikken and Olvera de la Cruz 10.1073/pnas.1302406110

SI Text

Details Algorithm. We developed an algorithm to calculate the anisotropic pair-correlation functions and mean densities by means of the anisotropic hyper-netted chain. The dimension of the pair-correlation functions can be reduced from six to three thanks to the translational symmetry in the direction parallel to the boundaries: $h(\mathbf{x}, \mathbf{x}') = h(r, z, z')$. First, the z coordinate is discretized, and the Ornstein–Zernike equation (Eq. 3) is considered as a matrix equation, where each matrix element of the pair-correlation matrices corresponds to two z coordinates, $h_{ij}(r) = h(r, z_i, z_j)$. An interpretation of the method is shown in Fig. S1. Typically, we divide the r axis and z axis in 40–100 grid points each, such that the pair-correlation functions store up to 10^6 numbers. We defined a shorter-ranged direct correlation function $c_{ij}^*(r) \equiv c_{ij}(r) + \beta u_{ij}^*(r)$ to be able to perform the Hankel transformation over a shorter domain. The function $u_{ij}^*(r)$ is the Coulomb potential between two particles with z coordinates z_i and z_j and distance r parallel to the boundary, with a correction for large values near the origin for $i \sim j$. The function is introduced purely for mathematical/numerical convenience and not an approximation in the theory. To numerically solve the Ornstein–Zernike equation (Eq. 3), we Hankel-transform the matrix elements $h_{ij}(r)$ of the total correlation function matrix and solve an algebraic matrix equation in k space to obtain the direct correlation functions. The direct correlation functions are consequently used to calculate the new total correlation functions by using the hyper-netted chain closure (Eq. 4) without the bridge function and a term $u_{ij}(r) - u_{ij}^*(r)$, setting straight our rescaling of c that was performed for numerical convenience during the Hankel transformations and a convenient inclusion of the image charge effects. Iteratively, we calculate the density profile (Eq. 5), which requires the pair-correlation functions as an input, and the pair-correlation functions, which require the density as an input. The iteration is continued until a self-consistency is obtained with a relative precision of typically 10^{-8} . A simple Picard iteration scheme sufficed for convergence in 1 min to 2 h on a single CPU. To optimize the efficiency of the code, we typically chose an r range of 4–5 Debye lengths or bulk correlation lengths. Both the routines for the matrix inversion and the Hankel transformation were obtained from the GNU scientific library. More background and a very detailed discussion can be found in refs. 1 and 2, which have been very helpful during the development.

Method of Images. As explained in ref. 1, the introduction of the correlation function c^* also has the advantage that it facilitates the method of images. The image contributions to the pair interactions need only be known in k space in the evaluation of the $\hat{c}_{ij}^*(k)$ from the Ornstein–Zernike equation. In the evaluation of $h_{ij}(r)$ from the hyper-netted chain closure, the contributions are cancelled out because of the term $u_{ij}(r) - u_{ij}^*(r)$. In k space, the contribution can be given analytically by explicit terms, which can be evaluated before the iteration procedure. The electrostatic pair potential between two particles consists of a direct contribution and the interactions with the images, which can be summed as follows. Every time a charge is reflected by the boundary between phase 1 and phase 2 or 3, its charge is modified by a factor A_{12} or A_{13} , respectively, such that the total Coulomb potential is a summation,

$$\beta u_{ij}(r) = q_i q_j l_B \left(\frac{1}{\sqrt{(z_i - z_j)^2 + r^2}} + \sum_{n=1}^{\infty} \frac{2A_{12}^n A_{13}^n}{\sqrt{(z_i - z_j + 2nH)^2 + r^2}} + \frac{2A_{12}^n A_{13}^n}{\sqrt{(z_j - z_i + 2nH)^2 + r^2}} + \sum_{n=0}^{\infty} \frac{A_{12}^n A_{13}^{n+1}}{(2z_M - z_i - z_j + 2nH)^2 + r^2} + \frac{A_{12}^{n+1} A_{13}^n}{(z_i + z_j - 2z_0 + 2nH)^2 + r^2} \right), \quad [\text{S1}]$$

that includes the direct interaction (first line), the even number of reflections (second line), and the odd number of reflections (third line). The boundaries are located at $z = z_0$ and $z = z_M$. After the Hankel-transform, the summation reads

$$\beta \hat{u}_{ij}(k) = \frac{2\pi q_i q_j l_B}{k} \left(e^{-|z_i - z_j|k} + \sum_{n=1}^{\infty} 2A_{12}^n A_{13}^n e^{-(z_i - z_j + 2nH)k} + 2A_{12}^n A_{13}^n e^{-(z_j - z_i + 2nH)k} + \sum_{n=0}^{\infty} A_{12}^n A_{13}^{n+1} e^{-(2z_M - z_i - z_j + 2nH)k} + A_{12}^{n+1} A_{13}^n e^{-(z_i + z_j - 2z_0 + 2nH)k} \right) \quad [\text{S2}]$$

and can be performed by recognizing the geometric series, leading to

$$\beta \hat{u}_{ij}(k) = \frac{2\pi q_i q_j l_B}{k} \left(e^{-|z_i - z_j|k} + \frac{2A_{12}A_{13}}{1 - A_{12}A_{13}e^{-2Hk}} \left(e^{-(z_i - z_j + 2Hk)k} + e^{-(z_j - z_i + 2Hk)k} \right) + \frac{1}{1 - A_{12}A_{13}e^{-2Hk}} \left(A_{13}e^{-(2z_M - z_i - z_j)k} + A_{12}e^{-(z_i + z_j - 2z_0)k} \right) \right). \quad [\text{S3}]$$

The notation of the second line of Eq. S3 can be simplified even further by recognizing a hyperbolic cosine, but it is not done in the algorithm for numerical safety to avoid multiplication of an extremely small number with an extremely large number. The self-interactions with the images (Eqs. 1 and 2) can be considered as an additional external potential that needs to be evaluated only one time in r space.

The image contributions are large if the factors A_{12} and A_{13} approach one (i.e., when the dielectric contrast is large between phase 1 and phases 2 and 3). The divergence in the limit of $A_{12} = A_{13} = 1$ is, in reality, avoided by the finite polarizability and thickness of the boundaries between two fluids or a fluid and a solid, but large values of the potential can be encountered, especially near the boundaries, and require extra care in the numerical algorithm (e.g., by adapting the function u^* near the boundary).

Some variations in the algorithm have been made, including annealing procedures, to deal with strong interactions (e.g., by lowering the temperature gradually, selectively increasing the ion charge, or changing the size of the ion or the dielectric constants to the desired value).

1. Kjellander R, Marčelja S (1984) Correlation and image charge effects in electric double layers. *Chem Phys Lett* 112(1):49–53.

2. Kjellander R, Marčelja S (1985) Inhomogeneous coulomb fluids with image interactions between planar surfaces. I. *J Chem Phys* 82(4):2122–2135.

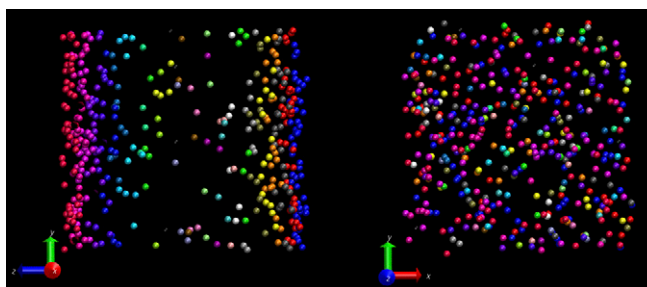


Fig. S1. From a perspective along the z axis, the inhomogeneous system (*Left*) appears homogeneous (*Right*). One can map the 3D inhomogeneous system to a 2D homogeneous system without loss of information about the coordinate that is lost by projection by labeling the particles in parallel layers as a distinct species. One exchanges inhomogeneity for polydispersity.

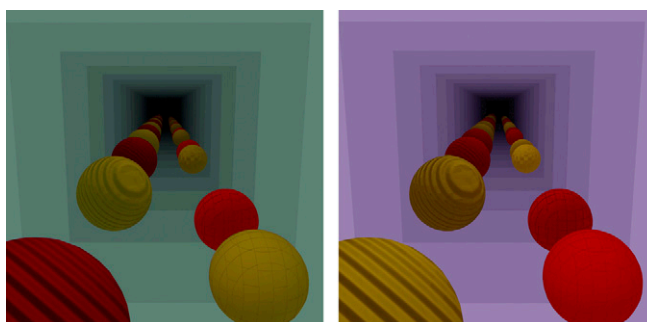


Fig. S2. Visualization of the method of images applied to a system of two charges that are confined between two parallel dielectric boundaries. Two conducting boundaries, or two boundaries with a stronger dielectric medium, invert the charge with every reflection, resulting in an alternating pattern of positive and negative image charges (*Left*; teal mirrors). Two different boundaries, one with a positive and one with a negative dielectric jump, invert and mirror the charge subsequently, resulting in a pattern where two negative images are followed by two positive ones and vice versa (*Right*; purple mirrors). The total electrostatic potential is obtained by summing the interactions between all of the images, which can be done conveniently in Fourier space as shown above.